

The Jahn–Teller Effect: A Case of Incomplete Theory for d^4 Complexes?

Jorge David,[†] Doris Guerra,[‡] and Albeiro Restrepo^{*‡}

[†]*Escuela de Ciencias y Humanidades, Departamento de Ciencias básicas, Universidad Eafit AA 3300, Medellín, Colombia, and* [‡]*Grupo de Química–Física Teórica, Instituto de Química, Universidad de Antioquia, AA 1226 Medellín, Colombia*

Received October 8, 2010

We present relativistic calculations at the four-component Dirac–DFT level for the geometries of the series of group 9 monoanionic hexafluorides MF_6^- , $M = \text{Co, Rh, Ir}$. Highly correlated four-component relativistic CCSD(T) energies were also calculated for the optimized geometries. Spin–orbit coupling effects influence the geometrical preferences for molecular structures: relativistic calculations predict ground states with octahedral symmetries O_h^* for all hexafluorides in this study, while at the nonrelativistic limit, a structural deviation toward D_{4h} ground state symmetries is predicted. Our findings suggest that relativistic effects have an important role in molecular structure preferences for the title hexafluorides.

Introduction

Crystal field theory (CFT) predicts that the hexafluorides of transition metals with $t_{2g}^4 e_g^0$ electron configuration exhibit triplet $^3T_{2g}$ ground states, which are prone to Jahn–Teller (JT) distortions or to splitting of the degenerate nonbonding molecular orbitals due to spin–orbit (SO) coupling effects.^{1,2} JT distortions of hexacoordinated transition metals are well-known,² especially when the t_{2g} orbitals in an octahedral environment are not fully occupied. To date, no one has postulated a relativistic JT theorem; therefore, molecular geometry distortions due to the dynamic JT effect are a consequence of nonrelativistic treatments. Complex combinations of JT effects and SO splittings are necessary to correctly describe molecular geometries.^{3,4} Many reports have dealt with JT and SO effects in octahedral hexafluorides;^{2,5–8} however, complications not encountered in the first transition series arise for $4d$ and especially for $5d$ complexes. The chief obstacle is the spin–orbit coupling, which is significant and comparable in magnitude to D_q , the crystal field splitting parameter for the square bipyramid, D_{4h}

geometries.⁹ Such large magnitudes should prevent the SO couplings from being treated as small perturbations for $5d$ transition metal complexes. Historically, the most popular theoretical approach to problems dealing with combined JT and SO effects avoids solution of the full relativistic Dirac Hamiltonian by diagonalizing the vibronic Hamiltonian (linear, quadratic JT) and then including the SO couplings via perturbations. Berckholtz and Miller have used this methodology to study molecules exhibiting C_{3v} geometries.¹⁰ They concluded, “the necessity of performing the complete calculation becomes clear as the deviations between approximation and reality becomes large.” A more sophisticated approach used by Domcke and co-workers in the treatment of trigonal symmetry molecules involves the vibronic Hamiltonian describing linear Jahn–Teller and spin–orbit couplings in the diabatic spin–orbital representation, employing the Breit–Pauli spin–orbit coupling operator in the single-electron approximation.¹¹ To our knowledge, there are no reports of attempts to include the SO coupling effects by solving the full relativistic Dirac Hamiltonian in the four-component space. Earlier experimental studies obtained SO couplings for $5d$ complexes from fitted extrapolations of the Tanabe–Sugano diagrams; the electronic spectra of IrF_6^- , an Ir(V) complex, were treated in this fashion.^{9,12}

Second and third row transition metal hexafluorides of group 10 prefer square bipyramid, D_{4h} , ground state geometries over O_h octahedral configurations in the absence of relativistic effects.¹ For the hexafluorides of group 10, molecular geometries are somewhat sensitive to relativistic effects for the second transition row (PdF_6), while inclusion

*To whom correspondence should be addressed. E-mail: albeiro@matematicas.udea.edu.co.

(1) David, J.; Fuentealba, P.; Restrepo, A. *Chem. Phys. Lett.* **2008**, 457, 42.

(2) Molski, M.; Seppelt, K. *Dalton Trans.* **2009**, 3379.

(3) Dyall, K.; Faegri, K. *Introduction to Relativistic Quantum Chemistry*; Oxford University Press: New York, 2007; p 467.

(4) Bersuker, I. *The Jahn–Teller Effect*; Cambridge University Press: Cambridge, U.K., 2010.

(5) Moffitt, W.; Goodman, G.; Fred, M.; Weinstock, B. *Mol. Phys.* **1959**, 2, 109.

(6) Weinstock, B.; Claassen, H. *J. Chem. Phys.* **1959**, 31, 262.

(7) Weinstock, B.; Claassen, H.; Malm, J. *J. Chem. Phys.* **1960**, 32, 181.

(8) Alvarez-Thon, L.; David, J.; Arratia-Pérez, R.; Seppelt, K. *Phys. Rev. A* **2008**, 77, 034502.

(9) Allen, G.; El-Sharkawy, G.; Warren, K. *Inorg. Chem.* **1972**, 11, 51.

(10) Berckholtz, T.; Miller, T. *Int. Rev. Phys. Chem.* **1998**, 17, 435.

(11) Domcke, W.; Mishra, S.; Poluyanov, L. *Chem. Phys.* **2006**, 322, 405.

(12) Brown, D.; Russell, D.; Sharp, D. *J. Chem. Soc. A* **1966**, 18.

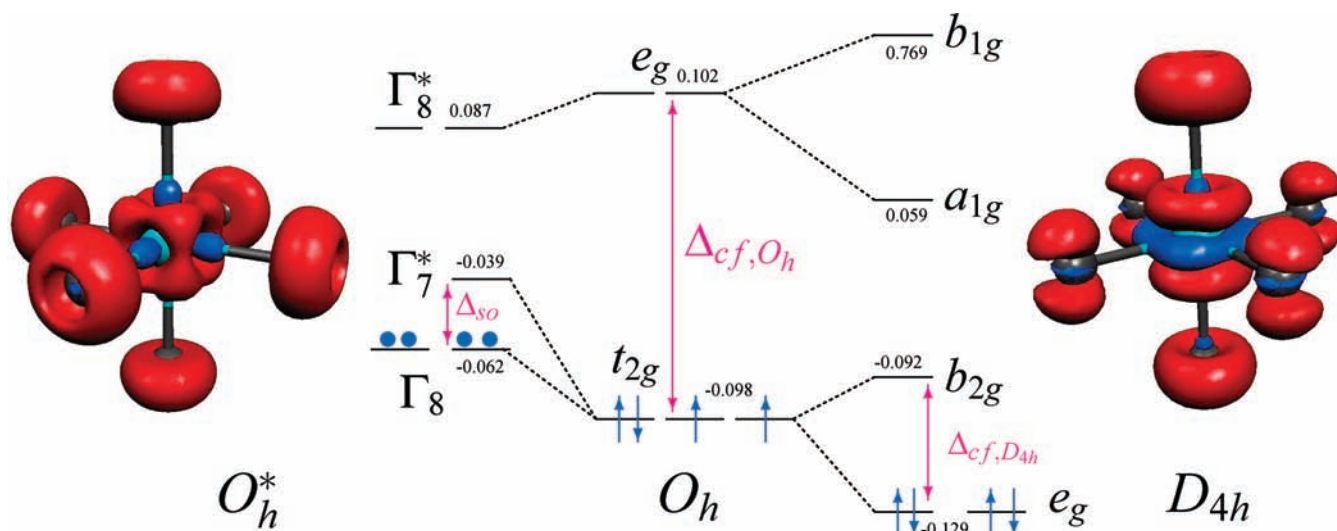


Figure 1. Effects of relativity on the geometries, shapes of the HOMOs, and orbital splittings for the MF_6^- series. Nonrelativistic calculations predict singlet, e_g^4 , D_{4h} geometries. Crystal field theory predicts triplet t_{2g}^4 , O_h geometries. Our four-component relativistic calculations predict singlet γ_8^4 , O_h^* geometries. A dramatic difference in the shape of the HOMO is observed for the distorted D_{4h} geometry, showing large contributions from the p orbitals on the equatorial F atoms. Energy splittings are not drawn to scale to help visualization; orbital energies (au) for the IrF_6^- complex are shown as a guide.

of relativistic effects is mandatory for accurate descriptions of third row hexafluoride (PtF_6) geometries.¹ One interesting question that we address in this report is whether relativistic effects influence molecular geometries for transition metal hexafluorides as a general norm. Among the reported cases in which relativistic effects are needed for the correct prediction of molecular geometries, we cite a few: PdF_6 and PtF_6 ,¹ CH_2ICl^+ ,¹³ WF_5 ,¹⁴ and UF_5 .¹⁵

Theory

The Dirac–Coulomb relativistic Hamiltonian for an n -electron molecular system within the Born–Oppenheimer approximation is written in atomic units as

$$\mathcal{H}_{\text{DC}} = \sum_{i=1}^n h_{\text{D}}(i) + \sum_{i=1}^n \sum_{j>i}^n \frac{1}{r_{ij}} \quad (1)$$

where $h_{\text{D}}(i)$ is the one-particle Dirac Hamiltonian defined as

$$h_{\text{D}}(i) = c\alpha_i \cdot \mathbf{p}_i + (\beta_i - 1)c^2 + v(i) \quad (2)$$

with c being the speed of light, $v(i)$ the external potential, and α and β the four-dimensional Dirac matrices

$$\alpha_q = \begin{pmatrix} 0 & \sigma_q \\ \sigma_q & 0 \end{pmatrix}, q = x, y, z; \quad \beta = \begin{pmatrix} \mathbf{I}_2 & \mathbf{0}_2 \\ \mathbf{0}_2 & -\mathbf{I}_2 \end{pmatrix} \quad (3)$$

where \mathbf{I}_2 and $\mathbf{0}_2$ are two-dimensional unit and null matrices and σ_q represents the Pauli spin matrices. In the relativistic case, in the O_h^* double group symmetry, the extra irreducible representations for the d shell are determined by the direct products of the spin functions with the irreducible representations t_{2g} and e_g of the nonrelativistic O_h group

$$\Gamma_{\text{spin}} \otimes t_{2g} = \Gamma_8 \oplus \Gamma_7 \quad (4)$$

and

$$\Gamma_{\text{spin}} \otimes e_g = \Gamma_8 \quad (5)$$

where Γ_8 and Γ_7 are four- and two-dimensional extrairreducible representations, respectively (see Figure 1).

Computational Details

The Dirac08 suite of programs¹⁶ was used to optimize the molecular geometries of the molecular complexes MF_6^- ($M = \text{Co}, \text{Rh}, \text{Ir}$) at the four-component relativistic Dirac–DFT (LDA, B3LYP for electron exchange and correlation) level and in the nonrelativistic limit. The Dyall.cv2z basis sets^{17,18} were used for the metals; for the fluorine atom, the extended 6-311G* and 6-311+G* basis set were used. O_h octahedral geometries for all optimizations were used as initial guesses; the optimizations were carried out under the D_{2h} subgroup as implemented in Dirac08. The kinetic balance condition was used to obtain the small relativistic components of the basis set.^{19–22} Model interatomic SS-integral contributions by classical repulsion of small component atomic charges²⁵ was used in the optimizations. Four-component relativistic CCSD(T) single point energy calculations on the optimized geometries were carried out by considering the active spaces listed in Table 1. One common way to set the active spaces for highly correlated calculations is to include the molecular orbitals resulting from the combinations of all valence atomic spinors; another way is to consider only molecular orbitals falling between some energy cutoffs.^{23,24} In this work, we try

(16) Joergen, H.; Jensen, Aa.; Visscher, L. *Dirac08*; see <http://dirac.chem.sdu.dk> (accessed Dec 2010).

(17) Dyall, K. *Theor. Chem. Acc.* **2004**, *112*, 403.

(18) Dyall, K. *Theor. Chem. Acc.* **2007**, *117*, 483.

(19) Ishikawa, Y.; Binning, R.; Sando, K. *Chem. Phys. Lett.* **1983**, *101*, 111.

(20) Ishikawa, Y.; Binning, R.; Sando, K. *Chem. Phys. Lett.* **1983**, *105*, 189.

(21) Stanton, R.; Havriliak, S. J. *Chem. Phys.* **1984**, *81*, 1910.

(22) Visscher, L.; Visser, O.; Aerts, P. J. C.; Merenga, H.; Nieuwpoort, W. C. *Comput. Phys. Commun.* **1994**, *81*, 120.

(23) Malli, G. *Prog. Theor. Chem. Phys.* **2002**, *6*, 243.

(24) Malli, G.; Siegert, M.; Turner, D. *Int. J. Quantum Chem.* **2004**, *99*, 940.

(25) Visscher, L. *Theor. Chem. Acc.* **1997**, *89*, 68.

(13) Lee, M.; Kim, H.; Lee, Y.; Kim, M. *Angew. Chem., Int. Ed.* **2005**, *44*, 2929.

(14) Dyall, K. *J. Phys. Chem. A.* **2000**, *104*, 4077.

(15) Onoe, J.; Nakamatsu, H.; Mukoyama, T.; Sekine, R.; Adachi, H.; Takeuchi, K. *Inorg. Chem.* **1997**, *36*, 1934.

Table 1. Active Spaces for Relativistic CCSD(T) Calculations of the MF_6^- Hexafluorides

hexafluoride	spinor class		total number of allowed excited configurations		
	occupied	virtual	single	double	triple
CoF_6^-	42	40	1680	671580	1.134224×10^8
RhF_6^-	44	40	1760	737880	1.308507×10^8
IrF_6^-	84	40	3360	2719080	9.414059×10^8

Table 2. Four-Component Relativistic (Dirac–DFT) and Nonrelativistic M–F Bond Distances (Å) for the Group 9 Hexafluorides^a

metal	Dirac-LDA		O_h^*	D_{4h}		experiment
	6-311+G*	6-311G*	Dirac-B3LYP	axial	equatorial	
Co	1.738	1.733	1.751	1.805	1.736	
Rh	1.854	1.851	1.884	1.956	1.871	1.86(1) ²⁶
Ir	1.888	1.886	1.907	2.009	1.914	1.879(5) ²⁶

^a Experimental geometries are octahedral. D_{4h} nonrelativistic geometries at the B3LYP level using the 6-311G* basis set for F atoms and the Dyall.cv2z basis sets for the central cations.

to approach the variational limit by including as many excited configurations as possible during the relativistic CCSD(T) calculations (Table 1); in this way, we ensure that as much electron correlation as possible is included.

Results and Discussion

Two different experimental techniques have been reported for the molecular geometries of RhF_6^- and IrF_6^- : synchrotron X-ray powder diffraction data (SPDD)²⁶ and extended X-ray absorption fine structure (EXAFS).²⁷ All hexafluorides calculated here are predicted to have O_h^* octahedral equilibrium geometries under four-component relativistic optimizations, while the nonrelativistic limit calculations afford ground states with D_{4h} symmetries. Geometrical parameters are listed in Table 2. An excellent agreement between calculation and experiment is observed, with deviations no larger than 1.6% from the calculated bond lengths.

Table 2 shows significant differences between relativistic and nonrelativistic calculations; these results clearly show that relativistic effects (SO couplings) must be accounted for if a good description of the molecular geometries for the title species is desired. There is ~9% M–F relativistic bond length enlargement in the octahedral geometry on going from CoF_6^- to IrF_6^- , while at the nonrelativistic limit, molecular geometries distort from regular octahedra to axially elongated square bipyramids for all cases. There are ~10% and ~11% enlargements of the equatorial and axial M–F distances, respectively, on going from CoF_6^- to IrF_6^- . Figure 1 shows the energy splitting of the nonbonding molecular orbitals for all cases treated in this study and the splitting influence on the molecular geometries.

Relativistic binding energies for all hexafluorides are listed in Table 3. All complexes are thermodynamically very stable with respect to atomization. We point out that relativistic LDA does a poor job by severely overestimating binding energies; to a lesser extent, relativistic MP2 also overestimates binding energies, revealing the need for high levels of electron correlation for correct energy predictions in the group 9 hexafluorides.

Relativistic $\Gamma_8 \rightarrow \Gamma_8^*$ electron transitions for the IrF_6^- complex are predicted to occur in the vicinity of $\sim 32\,649\text{ cm}^{-1}$

Table 3. Four-Component Relativistic Binding Energies (au) for the MF_6^- Hexafluorides^a

hexafluoride	Dirac-LDA	RMP2	RCCSD	RCCSD(T)
CoF_6^-	−7.98	−5.84	−5.60	−5.63
RhF_6^-	−6.84	−2.20	−2.01	−2.04
IrF_6^-	−6.75	−2.02	−2.03	−2.04

^a All calculations using the 6-311G* basis set for F atoms and the Dyall.cv2z basis sets for the central cations.

at the Dirac–LDA level (Figure 1, Table 4); this result is in excellent agreement with experimental values for $d \rightarrow d$ charge transfer transitions of $\sim 30\,000\text{ cm}^{-1}$ and higher for neutral octahedral $5d$ complexes reported by Moffitt and co-workers.⁵ Jørgensen²⁸ assigned all $d \rightarrow d$ charge transfer bands in the $30\,000\text{--}40\,000\text{ cm}^{-1}$ range. Experimental $d \rightarrow d$ transitions are reported to be on the order of $32\,000\text{ cm}^{-1}$ for the isoelectronic PtF_6 complex, while Dirac–DFT calculations predict $31\,711\text{ cm}^{-1}$ for the same transitions.¹ For the IrF_6^- complex, an earlier treatment by Allen et al.⁹ reported a $10D_q \approx 28\,500\text{ cm}^{-1}$; the value was obtained by extrapolating the Racah parameters of the Tanabe–Sugano diagrams.²⁹

Table 4 shows that $\Delta_{\text{SO}\Gamma_8 \rightarrow \Gamma_8^*}$, the magnitude of the spin–orbit coupling effect, increases by factors of $\sim n$, $2n$, and $7n$ with the Z of the central metal atom as we go down group 9 ($\text{Co} \rightarrow \text{Rh} \rightarrow \text{Ir}$), n being the $\Delta_{\text{SO}\Gamma_8 \rightarrow \Gamma_8^*}$ for CoF_6^- . The absence of the large spin–orbit couplings predicted here leads to distortions of the octahedral geometries toward square bipyramid arrangements in the nonrelativistic limit. We emphasize the fact that the geometrical distortion is present in all nonrelativistic calculated group 9 hexafluorides, including CoF_6^- , Co being a relatively small Z nucleus; in other words, from the relativistic point of view, the geometrical distortion is largely due to the absence of SO coupling as opposed to the absence of kinetic energy corrections. It is necessary to point out that $\Delta_{\text{SO}\Gamma_8 \rightarrow \Gamma_8^*} \approx 752\text{ cm}^{-1}$ for CoF_6^- (Table 4) is relatively small; therefore, there could be competition between several spin states close in energy. This situation should be properly described by the use of multi-configuration methodologies. Nonetheless, the octahedral geometries predicted by our four-component Dirac–DFT

(26) Graudejus, O.; Wilkinson, A.; Chacón, L.; Bartlett, N. *Inorg. Chem.* **2000**, *39*, 2794.

(27) Brisdon, A.; Holloway, J.; Hope, E.; Levason, W. *Polyhedron* **1992**, *11*, 7.

(28) Jørgensen, C. *Absorption Spectra and Chemical Bonding in Complexes*; Pergamon Press: Oxford, U. K., 1962.

(29) Tanabe, Y.; Sugano, S. *J. Phys. Soc. Jpn.* **1954**, *9*, 753.

Table 4. Four-Component Relativistic Molecular Orbitals (RMOs, Figure 1) Energy Gaps in cm^{-1} Calculated at the Dirac-LDA Level^a

hexafluoride	$\Delta_{\text{SO}_{\Gamma_8 \rightarrow \Gamma_7^*}}$		$\Delta_{\Gamma_8 \rightarrow \Gamma_8^*}$		$\Delta_{\text{CF}_{e_g \rightarrow b_{2g}}}$
	6-311+G*	6-311G*	6-311+G*	6-311G*	6-311G*
CoF_6^-	749	754	19548	19841	8682
RhF_6^-	1614	1628	27119	27672	8164
IrF_6^-	5118	5106	32312	32649	8044

^a $\Delta_{\text{SO}_{\Gamma_8 \rightarrow \Gamma_7^*}}$ due to spin-orbit coupling, $\Delta_{\Gamma_8 \rightarrow \Gamma_8^*}$: (RLUMO + 1) – RHOMO gap, $\Delta_{\text{CF}_{e_g \rightarrow b_{2g}}}$ due to crystal field in D_{4h} symmetry (nonrelativistic limit). Pople style basis sets used for the F atoms and Dyall.cv2z basis sets used for the central cations.

calculations are consistent with the results for the heavier hexafluorides.

An interesting observation is that the magnitude of $\Delta_{\text{SO}_{\Gamma_8 \rightarrow \Gamma_7^*}}$ on the relativistic O_h^* geometries increases dramatically with the Z of the central cation (Figure 1, Table 4),

while the predicted crystal field splittings of the $5d$ orbitals in the distorted D_{4h} geometries in the nonrelativistic limit decrease with Z (Figure 1, Table 4).

The inclusion of diffuse functions in the basis sets to better treat the F^- anions seems to make little difference for calculated molecular geometries and energetics. Deviations because of the inclusion of such functions amount to no more than $\sim 0.3\%$ in bond lengths (Table 2) and $\sim 2\%$ in orbital energy splittings (Table 4).

Acknowledgment. This work has been supported by Universidad EAFIT, internal project number 173-000013, and by Universidad de Antioquia, internal project number CODI-IN579CE. Professor Julio Arce, Universidad del Valle, Colombia, gave us valuable insights while discussing this problem with us; his help is greatly appreciated.